PHYSICAL REVIEW B **96**, 041302(R) (2017)

Disorder-dependent valley properties in monolayer WSe_2

Kha Tran,[1] Akshay Singh,[1,*] Joe Seifert,[1] Yiping Wang,[1] Kai Hao,[1] Jing-Kai Huang,[2] Lain-Jong Li,[2] Takashi Taniguchi,[3] Kenji Watanabe,[3] and Xiaoqin Li[1,4,†]

[1]*Department of Physics and Center for Complex Quantum Systems, University of Texas at Austin, Austin, Texas 78712, USA*
[2]*Physical Science and Engineering Division, King Abdullah University of Science and Technology, Thuwal 23955, Saudi Arabia*
[3]*National Institute of Material Science, 1-1 Namiki, Tsukuba, Ibaraki 305-0044, Japan*
[4]*Texas Materials Institute, University of Texas at Austin, Austin, Texas 78712, USA*

(Received 27 February 2017; revised manuscript received 13 June 2017; published 18 July 2017)

We investigate the effect of disorder on exciton valley polarization and valley coherence in monolayer WSe_2. By analyzing the polarization properties of photoluminescence, the valley coherence (VC) and valley polarization (VP) are quantified across the inhomogeneously broadened exciton resonance. We find that disorder plays a critical role in the exciton VC, while affecting VP less. For different monolayer samples with disorder characterized by their Stokes shift (SS), VC decreases in samples with higher SS while VP does not follow a simple trend. These two methods consistently demonstrate that VC as defined by the degree of linearly polarized photoluminescence is more sensitive to disorder, motivating further theoretical studies.

DOI: 10.1103/PhysRevB.96.041302

Valley refers to energy extrema in electronic band structures. Valley pseudospin in atomically thin semiconductors has been proposed and pursued as an alternative information carrier, analogous to charge and spin [1–7]. In monolayer transition metal dichalcogenides (TMDs), optical properties are dominated by excitons (bound electron-hole pairs) with exceptionally large binding energy and oscillator strength [8,9]. These excitons form at the energy extrema K (K') points at the Brillouin zone boundary. Due to broken inversion symmetry in combination with time-reversal symmetry, the valley and spin are inherently coupled in monolayer WSe_2. Valley contrasting optical selection rules make it possible to optically access and control the valley index via exciton resonances as demonstrated in valley-specific dynamic Stark effect [10,11] as an example.

For valleytronic applications, particularly in the context of using valley as an information carrier, understanding both valley polarization and valley coherence is critical. Valley polarization represents the fidelity of writing information in valley index while valley coherence determines the ability to optically manipulate the valley index. Earlier experiments have demonstrated a high degree of valley polarization in photoluminescence (PL) experiments on some monolayer TMDs (e.g., MoS_2 and WSe_2), suggesting the valley polarization is maintained before excitons recombine [4–6,12]. Very recently, coherent nonlinear optical experiments have revealed a rapid loss of exciton valley coherence ($\sim$100 fs) in WSe_2 due to the intrinsic electron-hole exchange interaction [13]. The ultrafast dynamics associated with the valley depolarization ($\sim$1 ps) [14] and the even faster exciton recombination ($\sim$200 fs) [15,16] extracted from the nonlinear experiments are consistent with the PL experiments. As long as the valley depolarization and decoherence occurs on time scales longer or comparable with exciton recombination lifetime, the steady-state PL signal shall preserve polarization properties reflecting the valley-specific excitations.

It is important to ask the question if disorder potential influences valley polarization and coherence, considering the fact that there are still significant amount of defects and impurities in these atomically thin materials and the substrate. This critical question has been largely overlooked in previous studies. Here, we investigate how valley polarization and coherence change in the presence of disorder potential. First, valley coherence is observed to change systematically across the inhomogeneously broadened exciton resonance, while there is no clear trend in valley polarization. Valley properties of an exfoliated monolayer WSe_2 encapsulated between hexagonal boron nitride (hBN) layers show a plateau beyond the mobility edge within the exciton resonance. We suggest that this systematic change is related to exciton localization by disorder potential, where the low-energy side of the exciton resonance corresponds to weakly localized excitons and the high-energy side is associated with more delocalized excitons [17,18]. Furthermore, we investigated a number of monolayer WSe_2 samples with different defect density characterized by the Stokes shift (SS) between the exciton peak in photoluminescence and absorption. A higher degree of valley coherence is observed in samples with a smaller SS or lower defect density [19,20]. These two observations consistently suggest that shallow disorder potential reduces valley coherence. Our studies suggest that a more qualitative and systematic evaluation of valley coherence may guide the extensive ongoing efforts in searching for materials with robust valley properties.

The low-energy bands with associated spin configurations in monolayer WSe_2 are illustrated in Fig. 1(a). A dipole-allowed (i.e., an optically bright) transition can only occur if the electron in the conduction band and the missing electron in the valence band have parallel spins. Thus, the transition between the lowest conduction band and the highest valence band is dipole forbidden, and the lowest-energy bright exciton transition is between the second-lowest conduction band and the highest valence band as illustrated in Fig. 1(a). Using σ_+ (σ_-) polarized excitation light, excitons are preferentially

*Present address: Department of Material Science and Engineering, Massachusetts Institute of Technology, Cambridge, MA 02139, USA.
†elaineli@physics.utexas.edu

 ©2017 American Physical Society

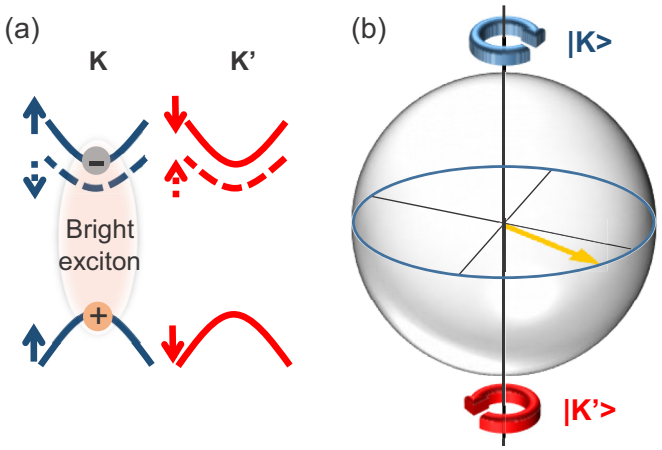

FIG. 1. (a) The band structure of monolayer WSe_2 at two degenerate K and K' valleys. A representative bright exciton transition is drawn at the K valley between the highest valence band and the second-lowest conduction band. Valley contrasting spins allow left (right) circular polarized light to excite excitons in the K (K') valley. The next highest valence band with opposite spin is separated by ~300 meV and is omitted for clarity. (b) Bloch sphere representation of valley pseudospin degree of freedom. Circular polarized light prepares an exciton in $|K\rangle$ or $|K'\rangle$ state, i.e., states at the poles, whereas linear polarized light prepares an exciton in a superposition of $|K\rangle$ and $|K'\rangle$, i.e., states at the equator.

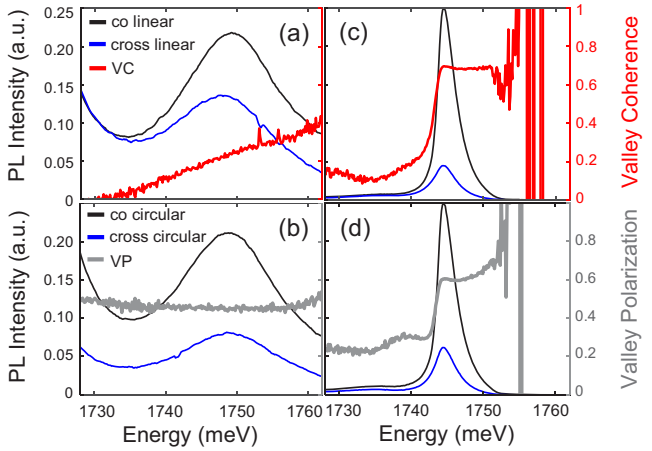

FIG. 2. (a) The exciton resonance shows co- (cross-) linear PL signal with respect to the linearly polarized excitation laser on an exfoliated WSe_2 monolayer (sample E5). Corresponding VC is plotted on the right vertical axis. (b) Co- and cross-circular polarized PL signal with respect to excitation polarization from the same sample in (a). The VP is plotted on the right vertical axis. (c) and (d) Same measurements are repeated for a hBN encapsulated monolayer (sample E1) WSe_2 with a much sharper exciton linewidth ~4 meV.

created in the K (K') valley due to the valley contrasting optical selection rules [1]. As with any binary quantum degree of freedom, K and K' valleys can be represented as a vector on a Bloch sphere, as shown in Fig. 1(b). The degree of valley polarization is defined by the normalized difference in cross-circular and cocircular signals as

$$\rho_{VP} = (I_{co} - I_{cross})/(I_{co} + I_{cross}), \quad (1)$$

where I_{co} (I_{cross}) represents co- (cross-) circular polarized PL intensity with respect to the excitation polarization. Previous studies on monolayer WSe_2 have reported a large valley polarization in steady-state PL experiments [13,21] suggesting that the valley scattering rate is slower or comparable with the exciton population recombination rate. In the Bloch sphere picture, a large valley polarization (VP) suggests that once the Bloch vector is initialized along the north pole, it retains its orientation during exciton population recombination time. On the other hand, when a linearly polarized excitation laser is used, a coherent superposition of two valley excitons is created [21]. Such a coherent superposition state corresponds to a Bloch vector on the equatorial circle. Previous experiments suggest that exciton valley coherence can be monitored by the linearly polarized PL signal [22,23]. Here, we follow this method and quantify the degree of valley coherence (VC) by the following definition:

$$\rho_{VC} = (I_{col} - I_{csl})/(I_{col} + I_{csl}), \quad (2)$$

where I_{col} (I_{csl}) represents co- (cross-) linear polarized PL intensity with respect to the excitation polarization.

We first investigate the change of VC and VP as a function of energy across the exciton resonance on mechanically exfoliated monolayer WSe_2 samples E1 [Figs. 2(c) and 2(d)] and E5 [Figs. 2(a) and 2(b)]. Sample E1 is a hBN encapsulated sample, while sample E5 is a bare monolayer on sapphire substrate. The list of all samples studied and their labels are provided in the Supplemental Material [24]. It is known that the degree of valley polarization depends strongly on the excitation wavelength [21,25]. In our experiments, the excitation energy is chosen to be energetically close to the exciton resonance to observe a finite degree of VC, but far enough so that resonant Raman scattering does not interfere with VC [21,25]. Unless mentioned otherwise, for all PL measurements presented in this Rapid Communication, we use a continuous-wave laser at 1.88 eV (i.e., 660 nm) and keep the power ~20 μW at the sample with a focused spot size of ~2 μm diameter. All measurements were performed at a temperature of ~13 K. A typical PL spectrum of monolayer WSe_2 exhibits two spectrally well resolved resonances corresponding to exciton and trion (a charged exciton), respectively (data included in the Supplemental Material [24]). There are two additional resonances at the lower energy, which may be due to either dark states or impurity bound states [26]. We focus on valley physics associated with the exciton resonance in this Rapid Communication.

Figure 2(a) plots the co- and cross-linear polarized PL, and the corresponding VC across the exciton resonance. The VC drops to zero at the lower-energy edge of the exciton resonance which spectrally overlaps with the trion resonance. Trions cannot exhibit VC in PL spectra due to photon-spin entanglement [21,27]. Interestingly, we observe a monotonic increase of the VC across the inhomogeneously broadened exciton resonance with ρ_{VC} varying from 0 to 0.4 as shown in Fig. 2(a). This monotonic change in VC across the exciton resonance is qualitatively repeated on all measured samples. VC reaches the maximum value at the high-energy side of the exciton and approaches zero at the low-energy end. We

suggest that the increase of VC across the exciton resonance arises from the degree of exciton localization [17,28,29].

In contrast, VP remains constant across the exciton resonance with $\rho_{VP} \sim 0.48$ as illustrated in Fig. 2(b). Previous studies suggested that only atomically sharp potentials can induce intervalley scattering and depolarization of valley excitons [21]. Thus, the nearly constant VP suggests that the inhomogeneously broadened exciton resonance is mainly due to slowly varying spatial potentials (in contrast to atomically sharp potentials). Such disorder potential may be attributed to local strain as well as shallow impurity potentials [17,28,29]. This speculation is also consistent with the observation that strongly localized excitons likely due to deep, atomically sharp potentials appear at much lower energy, ~100–200 meV below the exciton resonance [30,31]. An important mechanism causing valley depolarization is electron-hole exchange unaffected by shallow potential fluctuations [32–34]. Other valley scattering mechanisms such as D'yakonov-Perel' (DP) and Elliott-Yafet (EY) mechanisms are slower and considered unimportant for excitons in TMDs [32].

Next, we study the VP and VC of a hBN encapsulated monolayer WSe_2 with a narrow exciton PL linewidth of ~4 meV. Figures 2(c) and 2(d) plot the degree of valley coherence and valley polarization across the exciton resonance. We observe a very sharp rise of VC at the low-energy side of the exciton followed by a plateau of ~0.7 near the exciton peak and beyond. The VC plateau suggests that a mobility edge exists within the exciton resonance in this high-quality sample. At energy below the mobility edge, weakly localized excitons experience gradually varying disorder potential. Beyond the mobility edge, mostly delocalized excitons exhibit the same degree of VC. The qualitative feature of VP across the exciton resonance follows a similar trend, a rapid rise transitioning to a plateau of ~0.6 near the exciton peak. The rise of the VP in this sample is not consistent with the constant VP observed in other WSe_2 monolayer samples. It may arise from other low-energy resonances that are spectrally distinct in the encapsulated sample with a narrow exciton resonance.

To further investigate the role of disorder on valley properties, we studied a total of eight monolayer WSe_2 samples. We assume that the defect density is correlated with the spectral shift between exciton resonances measured in PL and absorption, known as the SS. As a simple method based entirely on commonly used linear optical spectroscopy methods, SS has been used to characterize a wide variety of systems [19,35] including defect density [36–38] and thickness fluctuations in quantum wells [20,39,40] and size distribution in ensembles of quantum dots [41,42].

A typical SS measurement is shown in Fig. 3(a). The PL and white light absorption spectra are taken from the same exfoliated monolayer WSe_2 labeled E5. The absorption spectrum is plotted as a differential and normalized spectrum $(T_s - T_m)/T_s$, where T_s is the transmission through the substrate and T_m is the transmission through both the substrate and the monolayer sample. The exciton resonances in the PL and absorption are fitted with Gaussian functions. The peaks extracted from the fittings are indicated by the dotted lines, yielding a 4.8 meV SS for this sample. As we increase the temperature from 13 K to room temperature, SS varies within

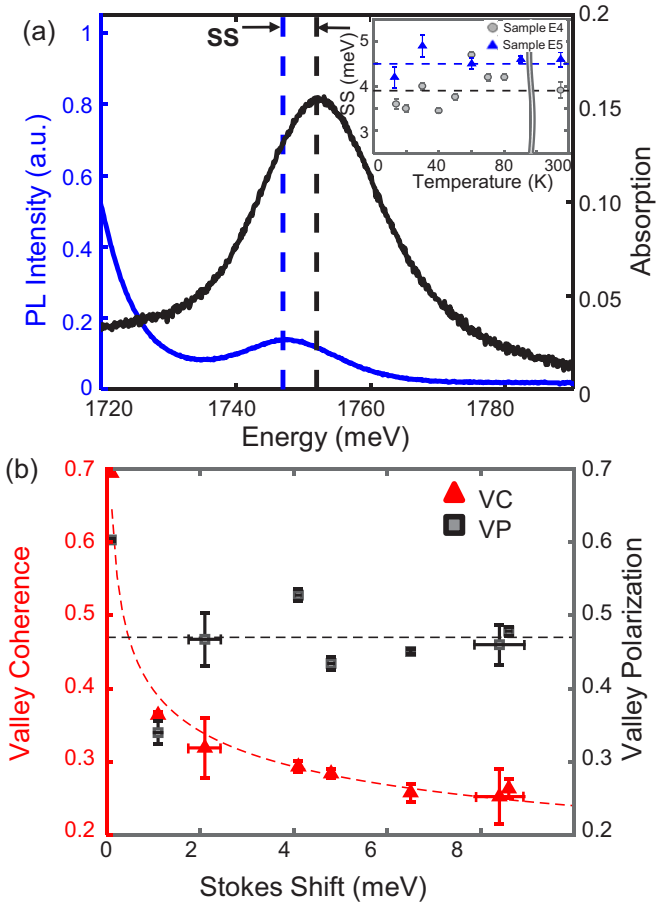

FIG. 3. (a) Stokes shift is shown as the difference in energy between the absorption spectrum and PL from the exciton resonance. Inset: SS dependence on temperature (b) VC (VP) is plotted with respect to SS. VC shows an inverse dependence versus SS, whereas VP shows no recognizable trend.

±0.6 meV [inset of Fig. 3(a)], which is within the error bars of our measurements.

To quantify the dependence of valley properties on SS (and on disorder potentials), the above measurements are repeated on all eight samples. For comparison across different samples, the VC (or VP) value for each sample is calculated by taking the average of the VC (or VP) in a range spanning $\pm\sigma/6$ from the exciton peak where σ is the fitted linewidth. We found the range of the spectral integration does not change our qualitative conclusion. Vertical error bars for VC (VP) in Fig. 3(b) are the standard deviation of the VC (VP) values. Horizontal error bars for SS in Fig. 3(b) are the sum of the fitting errors of the absorption spectrum and the PL spectrum. Some samples have small fitting errors and therefore their error bars are not visible within the plotted SS range. The results as summarized in Fig. 3(b) have a number of interesting features. Firstly, VC is found to decrease significantly with increasing SS of samples, with a fractional drop of ~64% between the samples with the lowest to highest SS. Specifically, ρ_{VC} varies from 0.69 to 0.25 as SS changes from 0 to 8.6 meV. Secondly, ρ_{VP} varies from 0.43 to 0.6 across the samples, and no clear correlation between VP and SS is observed. Based on the assumption that SS is correlated with the defect density in

different samples, we infer that disorder potential reduces VC but has no clearly identified systematic influence on VP. This conclusion is consistent with the spectral dependence of VC and VP across the exciton resonance observed on individual samples as reported in Figs. 2(a)–2(d). In addition, a recent experiment [28] investigated spatial variations of VP and VC on a chemical vapor deposition grown monolayer WSe_2. While VP was found to be mostly constant, VC showed significant changes, likely arising from disorder potential.

In summary, we report an experimental study of the effect of disorder on VC and VP in monolayer WSe_2. The low-energy side of the exciton resonance is associated with weakly localized excitons, and the high-energy side with more delocalized excitons. Using steady-state polarization resolved PL, we observe that the VC increases across the inhomogeneously broadened exciton resonance. In the highest-quality exfoliated sample encapsulated between hBN layers, a plateau of VC is reached at energy beyond a mobility edge within the exciton resonance. The existence of a mobility edge within exciton resonance and its effect on trion formation dynamics have been previously studied in monolayer $MoSe_2$ [17]. VP and VC are then measured for a number of samples with different SS (a measure of disorder). VC varies inversely with SS while no clear and systematic changes of VP have been observed across different samples. Our observations suggest that shallow disorder potentials have a crucial effect on the exciton valley coherence. Particularly, weakly localized excitons lose valley coherence more rapidly than the delocalized excitons. A recent theoretical study suggested that the exciton intervalley scattering time from disorder potential does not exhibit monotonic changes [43]. However, scattering time cannot be directly extracted from steady-state PL experiments reported here. Our work should motivate future experiments and microscopic theoretical studies necessary for a comprehensive understanding of the effect of disorder on valley properties in TMDs.

We gratefully acknowledge helpful discussions with Galan Moody and Fengcheng Wu. The spectroscopic experiments were jointly supported by NSF DMR-1306878 (A.S.) and NSF EFMA-1542747 (K.T., K.H., J.S., and X.L.). H.L. also gratefully acknowledges support from Welch Foundation Grant No. F-1662. K.W. and T.T. acknowledge support from the Elemental Strategy Initiative conducted by the MEXT, Japan and JSPS KAKENHI Grant No. JP15K21722.

[1] D. Xiao, G.-B. Liu, W. Feng, X. Xu, and W. Yao, Phys. Rev. Lett. **108**, 196802 (2012).
[2] J. Lee, K. F. Mak, and J. Shan, Nat. Nanotechnol. **11**, 421 (2016).
[3] K. F. Mak, K. L. McGill, J. Park, and P. L. McEuen, Science **344**, 1489 (2014).
[4] H. Zeng, J. Dai, W. Yao, D. Xiao, and X. Cui, Nat. Nanotechnol. **7**, 490 (2012).
[5] T. Cao, G. Wang, W. Han, H. Ye, C. Zhu, J. Shi, Q. Niu, P. Tan, E. Wang, B. Liu, and J. Feng, Nat. Commun. **3**, 887 (2012).
[6] G. Sallen, L. Bouet, X. Marie, G. Wang, C. R. Zhu, W. P. Han, Y. Lu, P. H. Tan, T. Amand, B. L. Liu, and B. Urbaszek, Phys. Rev. B **86**, 081301 (2012).
[7] R. Schmidt, A. Arora, G. Plechinger, P. Nagler, A. Granados del Águila, M. V. Ballottin, P. C. M. Christianen, S. Michaelis de Vasconcellos, C. Schüller, T. Korn, and R. Bratschitsch, Phys. Rev. Lett. **117**, 077402 (2016).
[8] K. F. Mak, C. Lee, J. Hone, J. Shan, and T. F. Heinz, Phys. Rev. Lett. **105**, 136805 (2010).
[9] A. Splendiani, L. Sun, Y. Zhang, T. Li, J. Kim, C. Y. Chim, G. Galli, and F. Wang, Nano Lett. **10**, 1271 (2010).
[10] E. J. Sie, J. W. McIver, Y.-H. Lee, L. Fu, J. Kong, and N. Gedik, Nat. Mater. **14**, 290 (2015).
[11] J. Kim, X. Hong, C. Jin, S.-F. Shi, C.-Y. S. Chang, M.-H. Chiu, L.-J. Li, and F. Wang, Science **346**, 1205 (2014).
[12] K. F. Mak, K. He, J. Shan, and T. F. Heinz, Nat. Nanotechnol. **7**, 494 (2012).
[13] K. Hao, G. Moody, F. Wu, C. K. Dass, L. Xu, C.-H. Chen, L. Sun, M.-Y. Li, L.-J. Li, A. H. MacDonald, and X. Li, Nat. Phys. **12**, 677 (2016).
[14] A. Singh, K. Tran, M. Kolarczik, J. Seifert, Y. Wang, K. Hao, D. Pleskot, N. M. Gabor, S. Helmrich, N. Owschimikow, U. Woggon, and X. Li, Phys. Rev. Lett. **117**, 257402 (2016).
[15] C. Poellmann, P. Steinleitner, U. Leierseder, P. Nagler, G. Plechinger, M. Porer, R. Bratschitsch, C. Schuller, T. Korn, and R. Huber, Nat. Mater. **14**, 889 (2015).
[16] G. Moody, C. Kavir Dass, K. Hao, C.-H. Chen, L.-J. Li, A. Singh, K. Tran, G. Clark, X. Xu, G. Berghäuser, E. Malic, A. Knorr, and X. Li, Nat. Commun. **6**, 8315 (2015).
[17] A. Singh, G. Moody, K. Tran, M. E. Scott, V. Overbeck, G. Berghäuser, J. Schaibley, E. J. Seifert, D. Pleskot, N. M. Gabor, J. Yan, D. G. Mandrus, M. Richter, E. Malic, X. Xu, and X. Li, Phys. Rev. B **93**, 041401(R) (2016).
[18] A. Hichri, B. Amara, A. Sabrine, and J. Sihem, arXiv:1609.05634.
[19] F. Yang, M. Wilkinson, E. J. Austin, and K. P. O'Donnell, Phys. Rev. Lett. **70**, 323 (1993).
[20] F. Yang, P. J. Parbrook, B. Henderson, K. P. O'Donnell, P. J. Wright, and B. Cockayne, Appl. Phys. Lett. **59**, 2142 (1991).
[21] A. M. Jones, H. Yu, N. J. Ghimire, S. Wu, G. Aivazian, J. S. Ross, B. Zhao, J. Yan, D. G. Mandrus, D. Xiao, W. Yao, and X. Xu, Nat. Nanoechnol. **8**, 634 (2013).
[22] Z. Ye, D. Sun, and T. F. Heinz, Nat. Phys. **13**, 26 (2017).
[23] G. Wang, X. Marie, B. L. Liu, T. Amand, C. Robert, F. Cadiz, P. Renucci, and B. Urbaszek, Phys. Rev. Lett. **117**, 187401 (2016).
[24] See Supplemental Material at http://link.aps.org/supplemental/10.1103/PhysRevB.96.041302 for Sec. I describes the absorption and polarization resolved photoluminescence optical setup. Section II provides a list of all samples: their labels, as well as their associated Stokes shift. Section III shows the plot of samples' Stokes shift versus the absorption linewidth. In Sec. IV, we subtract the trion contribution from exciton degree of valley coherence and show that exciton degree of valley coherence is unchanged after the subtraction. Section V is the discussion of an additional data point from the chemical vapor deposition (CVD) grown sample.
[25] G. Wang, M. M. Glazov, C. Robert, T. Amand, X. Marie, and B. Urbaszek, Phys. Rev. Lett. **115**, 117401 (2015).
[26] H. Dery and Y. Song, Phys. Rev. B **92**, 125431 (2015).

[27] K. Hao, L. Xu, F. Wu, P. Nagler, K. Tran, X. Ma, C. Schüller, T. Korn, A. H. MacDonald, G. Moody, and X. Li, 2D Mater. **4**, 025105 (2017).

[28] A. Neumann, J. Lindlau, L. Colombier, M. Nutz, S. Najmaei, J. Lou, A. D. Mohite, H. Yamaguchi, and A. Högele, Nat. Nanotechnol. **12**, 329 (2017).

[29] T. Jakubczyk, V. Delmonte, M. Koperski, K. Nogajewski, C. Faugeras, W. Langbein, M. Potemski, and J. Kasprzak, Nano Lett. **16**, 5333 (2016).

[30] A. Srivastava, M. Sidler, A. V. Allain, D. S. Lembke, A. Kis, and A. Imamoğlu, Nat. Nanotechnol. **10**, 491 (2015).

[31] Y.-M. He, G. Clark, J. R. Schaibley, Y. He, M.-C. Chen, Y.-J. Wei, X. Ding, Q. Zhang, W. Yao, X. Xu, C.-Y. Lu, and J.-W. Pan, Nat. Nanotechnol. **10**, 497 (2015).

[32] T. Yu and M. W. Wu, Phys. Rev. B **89**, 205303 (2014).

[33] M. Z. Maialle, E. A. de Andrada e Silva, and L. J. Sham, Phys. Rev. B **47**, 15776 (1993).

[34] A. Ramasubramaniam, Phys. Rev. B **86**, 115409 (2012).

[35] X. Qian, Y. Zhang, K. Chen, Z. Tao, and Y. Shen, Dyes Pigm. **32**, 229 (1996).

[36] S. Chichibu, J. Vac. Sci. Technol. B **16**, 2204 (1998).

[37] P. R. C. Kent and A. Zunger, Phys. Rev. Lett. **86**, 2613 (2001).

[38] S. Srinivasan, F. Bertram, A. Bell, F. A. Ponce, S. Tanaka, H. Omiya, and Y. Nakagawa, Appl. Phys. Lett. **80**, 550 (2002).

[39] L. C. Andreani, G. Panzarini, A. V. Kavokin, and M. R. Vladimirova, Phys. Rev. B **57**, 4670 (1998).

[40] O. Rubel, M. Galluppi, S. D. Baranovskii, K. Volz, L. Geelhaar, H. Riechert, P. Thomas, and W. Stolz, J. Appl. Phys. **98**, 063518 (2005).

[41] B. L. Wehrenberg, C. Wang, and P. Guyot-Sionnest, J. Phys. Chem. B **106**, 10634 (2002).

[42] A. Franceschetti and S. T. Pantelides, Phys. Rev. B **68**, 033313 (2003).

[43] T. Yu and M. W. Wu, Phys. Rev. B **93**, 045414 (2016).